Conflict between the identification of a cosmic neutrino source and the sensitivity to mixing angles in a neutrino telescope

Ggyoung-Riun Hwang* and Kim Siyeon+

Department of Physics, Chung-Ang University, Seoul 156-756, Korea

(Received 22 November 2007; revised manuscript received 17 October 2008; published 14 November 2008)

Neutrino fluxes at telescopes depend on both initial fluxes out of astronomical bursts and flavor mixing during their travel to the Earth. However, since the information on the initial composition requires better precision in mixing angles and vice versa, neutrino detection at telescopes cannot provide solutions to both problems by itself. Thus, a probability to be measured at long-baseline oscillation is considered as a complement to the telescope, and problems like source identification and parameter degeneracy are examined under a few assumptions.

DOI: 10.1103/PhysRevD.78.093008 PACS numbers: 14.60.Pq, 95.55.Vj, 98.70.Sa

I. INTRODUCTION

Cosmic neutrinos can be classified into stellar, galactic, and extragalactic neutrinos according to their astronomical source. Stellar neutrinos include solar and supernova neutrinos, whose energy scale is of order of 1–10 MeV since they are mainly produced by nuclear interaction. There are fair records in which they were identified as being from the Sun and SN1987A, and examined for oscillation and matter effects [1,2]. Ultrahigh energy (UHE; $\gtrsim 10^{18}$ eV) cosmic particles are regarded to have their origin in extragalactic source like active galactic nuclei (AGN) and some gamma ray bursts (GRB's). Mechanisms to accelerate protons to high energies have been searched, from $\mathcal{O}$(PeV) to the Greisen-Zatsepin-Kuzmin limit, in GRB's [3,4]. In astronomy, GRB's are detected once a day on average. If an accelerated proton produces a pion, about 20% of its energy is transferred to neutrinos, although more than one pion can be produced from a proton. Thus there are abundant sources of neutrinos whose energy is higher than 100 TeV [5].

Decays of pions, such as $\pi^+ \to \mu^+ + \nu_\mu \to e^+ + \nu_\mu + \nu_e + \bar{\nu}_\mu$ or $\pi^- \to \mu^- + \bar{\nu}_\mu \to e^- + \nu_\mu + \bar{\nu}_e + \bar{\nu}_\mu$, are the main processes of neutrino production. The initial neutrino flavor ratio can be determined, depending on the charges of pions and the energy loss rates of muons in the processes of pion decay. Whether pions are produced by pp or by $p\gamma$ collision, the charges of pions and the ratio of $\nu_e/\bar{\nu}_e$ are different. Although both pions and muons lose energy in the environment in which pions were borne, long-lived muons are more likely to interact with the environment before decaying. The pions that decay into neutrinos without muon decays are called "muon-damped sources" Such electromagnetic energy loss of muons for GRB's becomes significant when the energy of the γ ray E_γ is $\gtrsim 100$ TeV and, thus, the energy of the neutrino E_ν produced from the muon-damped source is $\gtrsim 1$ TeV [6]. The intensities of neutrinos in 10^{14} eV $< E < 10^{16}$ eV and higher energies were studied. Their model-independent upper bounds were predicted [4,7]. If the decay mode of a pion includes muon decay, it will be called simply the "pion source," in comparison with the muon-damped source. The initial neutrino composition $\Phi^0(\nu_e):\Phi^0(\nu_\mu):\Phi^0(\nu_\tau) = 1:2:0$ from the pion source is gradually replaced by the composition $\Phi^0(\nu_e):\Phi^0(\nu_\mu):\Phi^0(\nu_\tau) = 0:1:0$ from the muon-damped source when the energy increases, passing about 1 TeV [6,8]. When the main source of neutrino production in the atmosphere is pion decay, the shift of the ratio $\Phi^0(\nu_\mu)/\Phi^0(\nu_e)$ from 2 to infinity according to increasing energy [9,10] was tested in the Super-Kamiokande experiment (SK) [11,12]. The transition in the flavor ratio can naturally be assumed to occur in the region of GRB's, and the corresponding aspect was discussed in Ref. [6]. The relative flavor ratios of detected fluxes vs energy exhibit saturation and transition. The saturation of $\Phi^t(\nu_\mu)/\Phi^t(\nu_e)$ close to 1 implies that the beam originated from a pion source for lower energy, while the transition of $\Phi^t(\nu_\mu)/\Phi^t(\nu_e)$ to a larger ratio implies that the beam includes a portion of a muon-damped source for higher energy.

There are a few neutrino telescopes under construction, which can detect high energy neutrinos of $E_\nu > 0.1$ TeV, e.g., IceCube [13], Antares [14], etc. They are designed to detect very high energy and UHE neutrinos and to distinguish a flavor from others. With a future Cerenkov detector, ν_μ is easy to detect due to the long tracks of muons, while ν_τ is distinguishable from ν_e by a double-bang event only near the PeV range. At $\mathcal{O}$(PeV), the neutrino telescopes will be able to observe double showers of ν_τ (one due to τ production and the other due to τ decay) and a W^- resonant event at 6.3 PeV that identifies $\bar{\nu}_e$ [15].

For cosmic neutrinos, the oscillation factor in a transition probability is averaged out due to long-distance travel and high frequency. Thus, the telescope experiment can provide effective measurements of mixing parameters,

*galaraja@phys.cau.ac.kr
+siyeon@cau.ac.kr

given that the neutrino flavor ratio at the source is known [16]. The current data of mixing parameters are phrased by the ranges in the magnitude of Pontecorvo-Maki-Nakagawa-Sakata (PMNS) elements,

$$|U_{\mathrm{PMNS}}| = \begin{pmatrix} 0.79\text{–}0.86 & 0.50\text{–}0.61 & 0\text{–}0.20 \\ 0.25\text{–}0.53 & 0.47\text{–}0.73 & 0.56\text{–}0.79 \\ 0.21\text{–}0.51 & 0.42\text{–}0.69 & 0.61\text{–}0.83 \end{pmatrix} \quad (1)$$

at the 3σ level [17]. This matrix implies the following values for individual parameters: $\Delta m^2_{21} = (7.1\text{–}8.9) \times 10^{-5}$ eV^2, $|\Delta m^2_{31}| = (2.2\text{–}3.0) \times 10^{-3}$ eV^2, $\sin^2\theta_{12} = 0.24\text{–}0.40$, $\sin^2\theta_{23} = 0.34\text{–}0.68$, and $\sin^2\theta_{13} \leq 0.040$, all at the 3σ level [18]. The yet-undetermined neutrino parameters can be organized case by case. The first is normal hierarchy (NH) or inverse hierarchy (IH): the sign of $\Delta m^2_{31} \equiv m^2_3 - m^2_1$ is unknown while the global best fit is obtained as $|\Delta m^2_{31}| = 2.6 \times 10^{-3}$ eV^2. Second, the sign of $\theta_{23} - \pi/4$, i.e., whether the majority of ν_τ is heavier (ν_3 for NH) or lighter (ν_2 for NH), is unknown. Third, a certain value of oscillation probability has an infinite number of candidate combinations of θ_{13} and δ_{CP} [19,20]. The ambiguity due to the above degeneracies needs to be clearly distinguished from that due to uncertainties.

In Sec. II, the probability of a neutrino oscillation is reviewed, focusing on how the degeneracies are generated and which oscillation experiment each mixing angle is most sensitive to. In Sec. III, we examine the sensitivities of neutrino fluxes to neutrino mixing angles. In Sec. IV, we discuss a few points about parameter degeneracies and source identification, where the data of neutrino telescopes are considered in company with the data of a long-baseline (LBL) oscillation under assumptions. Concluding remarks follow in Sec. V.

II. REVIEW ON DEGENERATE PROBABILITY OF OSCILLATION

The probability of neutrino oscillation may be degenerate because different sets of parameters result in the same value. For example, the probability of transition from ν_α to ν_β in two-neutrino oscillation with a single mixing angle and a single mass-squared difference Δm^2,

$$P_{\alpha\beta} = \delta_{\alpha\beta} - (2\delta_{\alpha\beta} - 1)\sin^2 2\theta \sin^2\left(\frac{\Delta m^2 L}{4E}\right), \quad (2)$$

is invariant under switching the sign of Δm^2 or changing the angle θ with its complementarity angle $\pi/2 - \theta$. Since the two sets, $(\theta, \Delta m^2)$ and $(\pi/2 - \theta, -\Delta m^2)$, are not physically different, the above probability is twofold degenerate simply due to $(\theta, \Delta m^2)$ and $(\pi/2 - \theta, \Delta m^2)$ or due to $(\theta, \Delta m^2)$ and $(\theta, -\Delta m^2)$.

The oscillation probability extended to three neutrinos in vacuum,

$$P_{\alpha\beta} = \delta_{\alpha\beta} - 4\sum_{i=1}^{2}\sum_{j=i+1}^{3} \mathrm{Re}[U_{\alpha i}U^*_{\beta i}U^*_{\alpha j}U_{\beta j}]\sin^2\left(\frac{\Delta m^2_{ji}L}{4E}\right) \pm 2\sum_{i=1}^{2}\sum_{j=i+1}^{3} \mathrm{Im}[U_{\alpha i}U^*_{\beta i}U^*_{\alpha j}U_{\beta j}]\sin\left(\frac{\Delta m^2_{ji}L}{2E}\right), \quad (3)$$

is given in terms of a 3×3 unitary transformation matrix U and three mass-squared differences $\Delta m^2_{ji} \equiv m^2_j - m^2_i$, where each of ν_α and ν_β may be one of ν_e, ν_μ, or ν_τ. In effect, $\Delta m^2_{31} \simeq \Delta m^2_{32}$ so they will not be distinguished hereafter. The PMNS matrix in standard parametrization is given by

$$U_{\alpha i} \equiv \begin{pmatrix} c_{12}c_{13} & s_{12}c_{13} & s_{13}e^{-i\delta} \\ -s_{12}c_{23} - c_{12}s_{23}s_{13}e^{i\delta} & c_{12}c_{23} - s_{12}s_{23}s_{13}e^{i\delta} & s_{23}c_{13} \\ s_{12}s_{23} - c_{12}c_{23}s_{13}e^{i\delta} & -c_{12}s_{23} - s_{12}c_{23}s_{13}e^{i\delta} & c_{23}c_{13} \end{pmatrix},$$

where s_{ij} and c_{ij} denote $\sin\theta_{ij}$ and $\cos\theta_{ij}$ with the mixing angle θ_{ij} between the ith and jth generations, respectively, and δ denotes a Dirac phase.

The degeneracy of the probability could stem from three mixing angles and three mass-squared differences. However, since a number of successful experiments found the values of some physical parameters, the possible multiplicity of degeneracy at present is at most 8. A twofold degeneracy in the eightfold has its origin in the ambiguity between a value of θ_{23} and its complementary angle, $\pi/2 - \theta_{23}$. The ν_μ-disappearance probability, which is the most sensitive to determine the value of θ_{23}, is expressed by [20]

$$1 - P(\nu_\mu \to \nu_\mu) = \sin^2 2\theta_{23}\cos^2\theta_{13}\sin^2\left(\frac{\Delta m^2_{31}L}{4E_\nu}\right) - \sin\left(\frac{\Delta m^2_{21}L}{4E_\nu}\right)\sin\left(\frac{\Delta m^2_{31}L}{4E_\nu}\right)\sin^2 2\theta_{23} \cdot (\cos^2\theta_{13}\cos^2\theta_{12} - \sin\theta_{13}\sin^2\theta_{23} \times \sin 2\theta_{12}\cos\delta), \quad (4)$$

where the leading two terms are invariant under the exchange of θ_{23} with its complementary angle. On the other hand, the ν_e-appearance probability with matter effect A,

$$P(\nu_\mu(\bar{\nu}_\mu) \to \nu_e(\bar{\nu}_e)) = \sin^2\theta_{23}\sin^2 2\theta_{13}\frac{\sin^2((\Delta m^2_{31} \mp A)L/4E_\nu)}{(1 \mp A/\Delta m^2_{31})^2} + \frac{\Delta m^2_{21}}{\Delta m^2_{31}}\sin 2\theta_{23}\sin 2\theta_{13}\sin 2\theta_{12}\cos(\delta \pm \Delta m^2_{31}L/4E_\nu)$$
$$\cdot\frac{\sin((\Delta m^2_{31} \mp A)L/4E)\sin(AL/4E_\nu)}{(1 \mp A/\Delta m^2_{31})(A/\Delta m^2_{31})} + \left(\frac{\Delta m^2_{21}}{\Delta m^2_{31}}\right)^2\cos^2\theta_{23}\sin^2 2\theta_{12}\frac{\sin^2(A/4E_\nu)}{(A/\Delta m^2_{31})^2}, \quad (5)$$

provides multiple solutions to the (θ_{13}, δ) pair and the $(\Delta m^2_{31}, \delta)$ pair, where $A \equiv 2\sqrt{2}G_F Y_e \rho E_\nu$ is given with a density ρ and an electron fraction Y_e [19,20]. The leading term in Eq. (5) is not sensitive to the sign of Δm^2_{31}, if the matter effect A is not significant. The second term is not indicative of the sign either, due to $\cos\delta$ and a suppressing factor $\Delta m^2_{21}/\Delta m^2_{31}$. So the $(\Delta m^2_{31}, \delta)$ pair causes another double degeneracy of the probability. This is well known as a matter of normal hierarchy or inverse hierarchy. The multiple possibilities in the pair of (θ_{13}, δ) for a value of $\sin 2\theta_{13}\cos\delta$ make up the eightfold degeneracy with two other double degeneracies.

If astronomical neutrinos from origins like GRB's or other types of extragalactic bursts are considered for the flavor transition, in the limit $L \to \infty$, the probability in Eq. (3) reduces to

$$P^t_{\alpha\beta} \to \delta_{\alpha\beta} - 2\sum_{i=1}^{2}\sum_{j=i+1}^{3}\mathrm{Re}[U_{\alpha i}U^*_{\beta i}U^*_{\alpha j}U_{\beta j}] \quad (6)$$

$$= \sum_{i=1}^{3}|U_{\alpha i}|^2|U_{\beta i}|^2. \quad (7)$$

Since the probability of a relatively long-distance oscillation compared to the wavelength is averaged out, the dependency on the sign of Δm^2_{ji} is hidden, so that the probability is blind to Δm^2_{ji}. Since it depends only on the absolute values of the elements in the PMNS matrix as shown in Eq. (7), its dependency on the phase δ is simply $\cos\delta$. Sensitive dependencies between other mixing angles and $P^t_{\alpha\beta}$ will be discussed in detail in Sec. IV.

Degeneracy problems arise because the number of effective measurements is not sufficient to specify all the physical parameters, and the forms of probabilities are multivariable sinusoidal functions. Here, the ambiguities from three types of degeneracies, the sign of Δm^2_{31} [21], the sign of $\pi/4 - \theta_{23}$ [22], and different pairs of (θ_{13}, δ)'s [23], will be clearly distinguished from the ambiguities from uncertainties. The degeneracy is a problem that causes ambiguity even when an average probability or an average flux without uncertainty is applied to determine the parameters. For more review, see Refs. [24].

III. LIMIT OF A NEUTRINO TELESCOPE

The initial flux of astronomical high energy neutrinos is assumed to be attributed to the decay of pions produced in $p\gamma$ collision. The relative ratio of neutrino flavors from pion decay is $\Phi^0(\nu_e):\Phi^0(\nu_\mu):\Phi^0(\nu_\tau) = 1:2:0$. If the daughter muon in pion decay does not decay due to the electromagnetic energy loss, the flavor ratio is changed into $\Phi^0(\nu_e):\Phi^0(\nu_\mu):\Phi^0(\nu_\tau) = 0:1:0$. So, the composition ratio $\Phi^0(\nu_\mu)/\Phi^0(\nu_e) = 2$ and its transition to infinity as the energy of neutrinos increases may occur in the region of GRB's, as it does in the atmosphere. However, it is impossible to estimate the initial flux of neutrinos as being produced in GRB's. But one can make this conjecture from detected fluxes at telescopes [25]. If the neutrino mixing is of tri-bimaximal type, as the simplest example, the pion source is identified by the flux ratio at telescopes $\Phi^t(\nu_e):\Phi^t(\nu_\mu):\Phi^t(\nu_\tau) = 1:1:1$, while the muon-damped source is identified by the flux ratio at telescopes 1:1.8:1.8. Thus, the transition in flavor ratios of detected fluxes at GRB's occurs with the relative ratio $\Phi^t(\nu_\mu)/\Phi^t(\nu_e)$ from 1 to 1.8 as the energy of neutrinos increases. In reality, it is impossible to determine, simply by reading results at telescopes, whether initial beams are pion sources or muon-damped sources, without any assumptions, for the following reasons: First, any information from astronomical neutrino bursts on the composition in a mixture of two types of sources cannot be obtained without using telescopes. Second, the mixing angles and masses still have uncertainties that are too broad to analyze the fluxes, and moreover, the fluxes to be detected at telescopes are significantly sensitive to mixing angles. Hereafter, we take a strong assumption, which is that a pion source and a muon-damped source can be distinguished, in order to illustrate the point of sensitivity to mixing angles.

Unless neutrinos decay, $\Phi^0(\nu_e) + \Phi^0(\nu_\mu) + \Phi^0(\nu_\tau) = \Phi^t(\nu_e) + \Phi^t(\nu_\mu) + \Phi^t(\nu_\tau)$ and $\sum_\alpha P^t_{\alpha\beta} = 1$, where $\Phi^t(\nu_\beta) = \sum_\alpha P^t_{\alpha\beta}\Phi^0(\nu_\alpha)$. Since relative fluxes at a telescope can be normalized such that $\sum_\alpha \Phi^0(\nu_\alpha) = \sum_\alpha \Phi^t(\nu_\alpha) = 1$, the normalized flux $\Phi^t(\nu_\alpha)$ is a linear combination of $P^t_{\beta\alpha}$'s, for example, $\Phi^t(\nu_\alpha) = P^t_{\mu\alpha}$ for a muon-damped source and $\Phi^t(\nu_\alpha) = 1/3(P^t_{e\alpha} + 2P^t_{\mu\alpha})$ for a pion source. The symmetric matrix $P^t_{\alpha\beta}$ in Eq. (7) has only three independent elements. Thus, when the initial condition of the neutrino beam is assumed such that both a pure pion source and a pure muon-damped source are allowed, $\Phi^t(\nu_\tau)$ and one of the following four fluxes may be unnecessary: $\Phi^t(\nu_e)$ from a pion source, $\Phi^t(\nu_\mu)$ from a pion source, $\Phi^t(\nu_e)$ from a muon-damped source, and $\Phi^t(\nu_\mu)$ from a muon-damped source. In reality, either $\Phi^t(\nu_e)$ or $\Phi^t(\nu_\mu)$ is more likely to be a mixed flux from a pion source and a muon-damped source, rather than a flux from a pure pion source or a pure muon-damped source. In

order to examine the sensitivities to mixing angles, however, we consider a pure pion source or a pure muon-damped source. Figures 1 and 2 illustrate the dependence of $\Phi^t(\nu_e)$ on θ_{23} and the dependence of $\Phi^t(\nu_\mu)$ on θ_{23}, respectively. For a given θ_{13}, the range of δ from 0 to 2π turns the curves into thick bands. The red (upper in Fig. 1 and lower in Fig. 2) and blue (lower in Fig. 2 and upper in Fig. 1) bands indicate the fluxes from a pure pion source or from a pure muon-damped source, respectively.

The symmetric probability in Eq. (7) has ranges estimated from the PMNS matrix at 3σ CL in Eq. (1),

$$P_{\alpha\beta} = \begin{pmatrix} 0.48\text{–}0.64 & 0.12\text{–}0.34 & 0.11\text{–}0.35 \\ \surd & 0.33\text{–}0.53 & 0.30\text{–}0.41 \\ \surd & \surd & 0.33\text{–}0.47 \end{pmatrix}. \quad (8)$$

Thus, the fluxes accompany nontrivial ranges. The plots in Figs. 1 and 2 illustrate the sensitivity of the fluxes to all the mixing angles, including the *CP* phase δ. The significant sensitivity to θ_{23} is expressed by the broad coverage in $\Phi^t(\nu_e)$ and $\Phi^t(\nu_\mu)$ of each colored stripe for fixed θ_{12} and θ_{13}. Each stripe is a bundle of curves for δ values from 0 to π. The top line of the stripe for $\Phi^t(\nu_e)$ indicates $\delta = 0$, while the bottom line of the stripe for $\Phi^t(\nu_\mu)$ indicates $\delta = 0$. Next, the sensitivity to θ_{12} was estimated only for $\delta = 0$ and $\delta = \pi$ and is illustrated by three kinds of lines outside the colored lines. It is clear that θ_{12} does not affect the fluxes as much as θ_{23} does. The θ_{13} dependency in the fluxes is illustrated by the widths of the flux stripes. A remarkable improvement in the precision of θ_{13} will be obtained from near future oscillation experiments, e.g., Daya Bay [26], Double CHOOZ [27], RENO [28], NOνA [29], and T2K [30]. In Figs. 1 and 2, two values of θ_{13} are used for comparison: 0.20 which is the current upper bound at 3σ CL, and 0.082 which is the upper bound at 3σ that RENO will accomplish. It is clearly illustrated that narrowing the stripes by a small bound of θ_{13} makes identifying the relative composition more realistic.

If a series of LBL oscillations, e.g., NOνA and T2K, are successful in achieving the aimed precision level, reducing the relative range of $\sin^2\theta_{23}$ at 3σ from 79% to 42% [31],

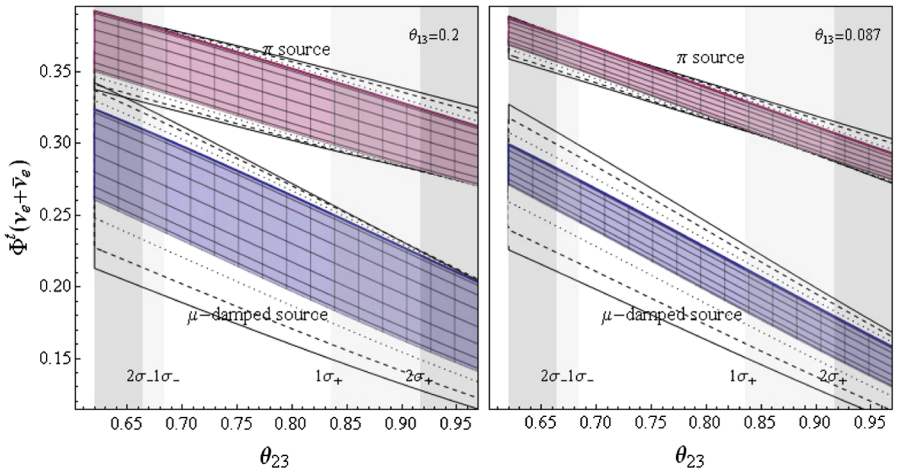

FIG. 1 (color online). $\Phi^t(\nu_e)$ vs θ_{23} for fixed values of θ_{13}.

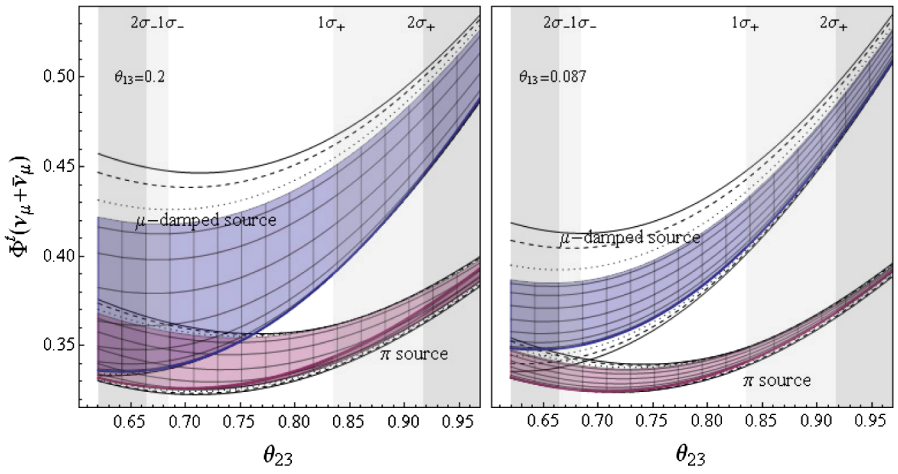

FIG. 2 (color online). $\Phi^t(\nu_\mu)$ vs θ_{23} for fixed values of θ_{13}.

the range in $\Phi^t(\nu_e)$ from a pure pion source is completely separated from the range in $\Phi^t(\nu_e)$ from a pure muon-damped source. The estimation of the composition rate in a mixed beam of two pure sources requires the determination of the CP phase δ as well as improved precision of other parameters.

The curves of neutrino fluxes with respect to energy show both saturation and transition. For instance, the initial flux ratio $\Phi^0(\nu_\mu)/\Phi^0(\nu_e)$ of atmospheric neutrinos saturates to 2 at the low energy limit [9,10], while the expected ratio $\Phi^t(\nu_\mu)/\Phi^t(\nu_e)$ of high energy cosmic neutrinos to be detected saturates to 1 at the low energy limit and to 1.8 at the high energy limit [6]. If we can distinguish the saturation from the transition in flux—energy plots—the identification of a neutrino beam from a pure pion source or a pure muon-damped source may be possible only after the accumulation of sufficient data of cosmic neutrino detection.

IV. LBL: A COMPLEMENT TO TELESCOPES

The probability $P_{\mu e}$ in Eq. (5) depends on $\cos(\delta + \Delta m^2_{31}L/4E_\nu)$, while $\Phi^t(\nu)$ in Eq. (7) depends on $\cos\delta$. If $\Phi^t(\nu)$ and $P_{\mu e}$ are the orthogonal axes as in Fig. 3, the locus of $\Phi^t(\nu)$ and $P_{\mu e}$ for δ from 0 to 2π completes a closed path. In Fig. 3, every locus in each figure passes a point in $P_{\mu e} - \Phi^t(\nu_e)$ space. The phrases $P(\nu_\mu \to \nu_e)$ and $\Phi(\nu_\alpha + \bar{\nu}_\alpha)$ in the figures are equivalent to $P_{\mu e}$ and $\Phi(\nu_\alpha)$ in the text. Especially in these figures, the probability $P_{\mu e}$ is an expected measurement of a super beam from J-PARC to Super-Kamiokande (T2K Collaboration). Thus, input values are adopted from Ref. [30]. The baseline L is 295 km and the energy of the neutrino, E_ν, is 1 GeV. The matter effect A in Eq. (5) is obtained with the Earth's density 2.8 g/cm^3 and the electron fraction 0.5. Equations (4) and (5) include only the leading terms.

A. Eightfold degeneracy

A number of strategies are proposed to solve the degeneracy problems by using the results of LBL oscillations and reactor neutrino oscillations in the future [19,24]. An example is to analyze long-baseline experiments over different oscillation distances [19], and another is to combine the results of reactor oscillations and the LBL [20]. This section checks possible resolutions obtainable from the combined analysis of results at telescopes and results at LBL.

The leading term of $P_{\mu e}$ in Eq. (5) with a remarkable sensitivity to θ_{13} does not distinguish $\Delta m^2_{31} > 0$ from $\Delta m^2_{31} < 0$ unless the matter effect is significant, and any detected flux $\Phi^t(\nu)$ is completely blind to Δm^2_{31}. However, the locus of $P_{\mu e}$ and $\Phi^t(\nu)$, as in Figs. 3 and 4, reveals the sign of the mass-squared difference Δm^2_{31} due to the phase difference $\Delta m^2_{31}L/4E_\nu$.

Each single curve in Fig. 3 is obtained from a set of specific values of θ_{23}, θ_{12}, and Δm^2_{31}, while δ runs from 0 to 2π. The value of θ_{12} is common for all curves in the figures, and there are two choices for each of θ_{23} and Δm^2_{31}: that θ_{23} may be a certain angle or its complementary angle, and that Δm^2_{31} may be $|\Delta m^2_{31}|$ or $-|\Delta m^2_{31}|$. Then, two sets of (θ_{13}, δ) exist for every set of $(\theta_{23}, \Delta m^2_{31})$, so that a total of eight pairs of (θ_{13}, δ)'s describe the point in $P_{\mu e} - \Phi^t(\nu_e)$ [24]. For instance, the point $(\Phi^t(\nu_e), P_{\mu e}) = (0.33, 0.010)$ in Fig. 3 intersected by the eight curves can be specified by the following eight pairs of (θ_{13}, δ) which belong to "a–h" curves:

a : (0.104, 2.3), b: (0.087, 3.8), c: (0.094, 2.4),
d: (0.079, 3.6), e: (0.086, 0.86), f: (0.071, 5.6),
g: (0.103, 1.01), h: (0.084, 5.4).

The above values of (θ_{13}, δ) are divided into two groups, according to θ_{23}: [a, b, c, d] for $\theta_{23} = \pi/4 - \epsilon$ and [e, f, g, h] for $\theta_{23} = \pi/4 + \epsilon$, where ϵ is a positive small angle. They can be divided also according to the sign of Δm^2_{31}: [a, b, e, f] for $\Delta m^2_{31} > 0$ and [c, d, g, h] for $\Delta m^2_{31} < 0$. In other words, the LBL oscillation probability $P_{\mu e}(\theta_{23} - \pi/4, \mathrm{sgn}(\Delta m^2_{31}), (\theta_{13}, \delta)) = 0.010$ is degenerated by the following eight possibilities:

$$\begin{aligned} P_{\mu e}(-\epsilon, +, \mathrm{a}) &= P_{\mu e}(-\epsilon, +, \mathrm{b}) = P_{\mu e}(-\epsilon, -, \mathrm{c}) \\ &= P_{\mu e}(-\epsilon, -, \mathrm{d}) = P_{\mu e}(+\epsilon, +, \mathrm{e}) \\ &= P_{\mu e}(+\epsilon, +, \mathrm{f}) = P_{\mu e}(+\epsilon, -, \mathrm{g}) \\ &= P_{\mu e}(+\epsilon, -, \mathrm{h}), \end{aligned} \tag{9}$$

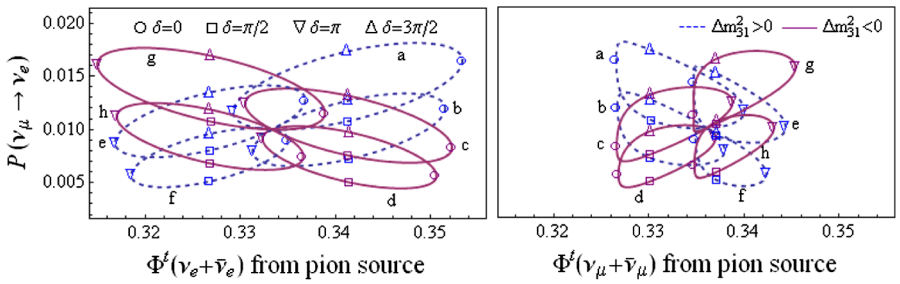

FIG. 3 (color online). Eight loci for $\delta \in [0, 2\pi]$ passing a common point in the $\Phi^t(\nu) - P_{\mu e}$ plane.

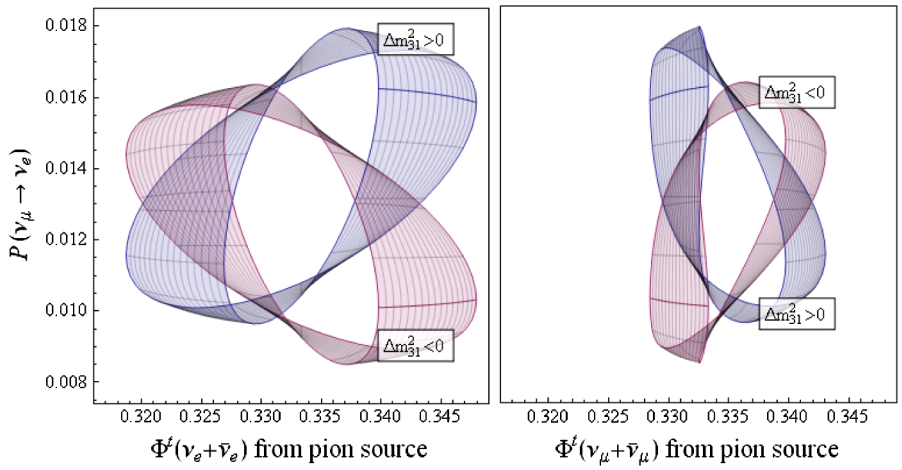

FIG. 4 (color online). Dependence of curves on Δm^2_{31}: θ_{12} is allowed within 3σ CL.

where $P_{\mu e}(-\epsilon, +, \mathrm{a})$, as an example, means that the probability is obtained when $\theta_{23} - \pi/4 = -\epsilon$, $\mathrm{sgn}(\Delta m^2_{31})$ is $+$, and (θ_{13}, δ) is the point on locus "a." Likewise, the flux at the telescope $\Phi^t(\nu_e)(\theta_{23} - \pi/4, \mathrm{sgn}(\Delta m^2_{31}), (\theta_{13}, \delta)) = 0.33$ is degenerated by the following eight possibilities:

$$\begin{aligned}\Phi^t(\nu_e)(-\epsilon, +, \mathrm{a}) &= \Phi^t(\nu_e)(-\epsilon, +, \mathrm{b}) = \Phi^t(\nu_e)(-\epsilon, -, \mathrm{c}) \\ &= \Phi^t(\nu_e)(-\epsilon, -, \mathrm{d}) = \Phi^t(\nu_e)(+\epsilon, +, \mathrm{e}) \\ &= \Phi^t(\nu_e)(+\epsilon, +, \mathrm{f}) = \Phi^t(\nu_e)(+\epsilon, -, \mathrm{g}) \\ &= \Phi^t(\nu_e)(+\epsilon, -, \mathrm{h}). \qquad (10)\end{aligned}$$

Thus, a point representing data from two experiments, e.g., the point $(\Phi^t(\nu_e), P_{\mu e}) = (0.33, 0.010)$ or the point $(\Phi^t(\nu_\mu), P_{\mu e}) = (0.34, 0.010)$ in Fig. 3, always belongs to many curves specified by different combinations of the parameters. The number of loci passing a point represents the order of degeneracy. In fact, the order of degeneracy becomes infinite if Δm^2_{31} or θ_{23} is allowed within a continuous range.

B. Breakable degeneracy by high energy cosmic neutrinos

Figure 4 displays the loci of $P_{\mu e}$ and $\Phi^t(\nu)$ for θ_{12} from 0.51 to 0.69 and δ from zero to 2π at $\theta_{13} = 0.010$ and $\theta_{23} = \pi/4$. The projections of the two bands onto the $\Phi^t(\nu)$ axis completely overlap with each other, and even the projections of the two bands onto the $P_{\mu e}$ axis mostly overlap with each other. So the individual measurement, either $\Phi^t(\nu)$ or $P_{\mu e}$, is not sensitive to the sign of Δm^2_{31}. However, the combination of two measurements as in Fig. 3 or Fig. 4 is significantly sensitive to whether $\Delta m^2_{31} > 0$ or $\Delta m^2_{31} < 0$. On the other hand, if θ_{23} and θ_{13} are also allowed within certain ranges rather than with fixed values, it is hard to get such distinct plots according to the type of mass hierarchy. Thus, an analysis with a fixed θ_{13} as in Fig. 4 can be effective only after a series of reactor or LBL neutrino oscillations, which will be launched ahead of neutrino detection at telescopes [26–30].

The leading term of $1 - P_{\mu\mu}$ in Eq. (4) is sensitive to θ_{23} but does not distinguish $\theta_{23} = \pi/4 - \epsilon$ from $\theta_{23} = \pi/4 + \epsilon$. On the other hand, the flux $\Phi^t(\nu_e)$ in Fig. 5, which is more sensitive to θ_{23} than the probability $P_{\mu e}$ is, shows a distinction of whether $\theta_{23} = \pi/4 - \epsilon$ or $\theta_{23} = \pi/4 + \epsilon$. Thus, $\Phi^t(\nu_e)$, which is a completely single-valued curve of θ_{23} in the currently allowed range as illustrated in Fig. 1 or in Fig. 5, avoids the degeneracy caused by the complementarity angle of θ_{23}, unlike $1 - P_{\mu\mu}$ in Eq. (4).

C. Source identification

Figure 5 is drawn under the assumption that the neutrino beam is purely from a pion source and purely from a muon-damped source. In reality, the initial flux from an astronomical burst is difficult to identify, whether the pion is produced in a $p\gamma$ collision or a pp collision and whether the initial condition is a pion source, a muon-damped source, or a mixture of them when a $p\gamma$ collision is dominant. Unlike the detection of photons at optical telescopes, the detection of neutrinos at telescopes should consider the change in neutrino flavors from the original outbursts. Moreover, broad uncertainties at present in neutrino mixing angles obstruct telescopes in describing the initial condition of neutrino beams.

The LBL oscillation probability $P_{\mu e}$ may again share a role in specifying the source of cosmic neutrinos. The shaded regions of both panels in Fig. 5 show the same area which both sources commonly cover. So the measurement of $\Phi^t(\nu_e)$ within the shaded region may indicate a beam from a pion source (right panel) for $\theta_{23} = 0.970$ or a beam from a muon-damped source (left panel) for $\theta_{23} = 0.623$. The distinction between them may be obtained by considering $P_{\mu e}$ together with $\Phi^t(\nu_e)$. For instance, Fig. 5

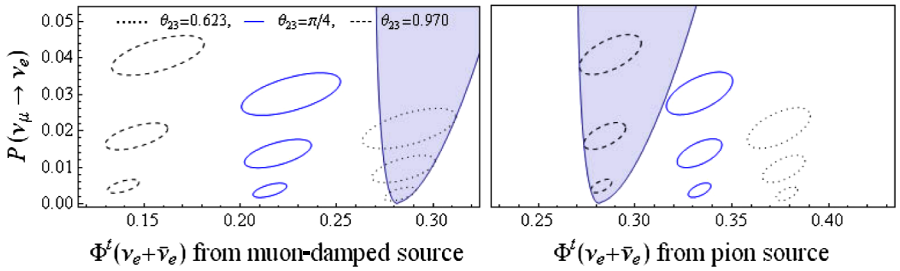

FIG. 5 (color online). The loci for $\delta \in [0, 2\pi]$ at $\theta_{13} = 0.15$, 0.10, or 0.05 for each θ_{23}.

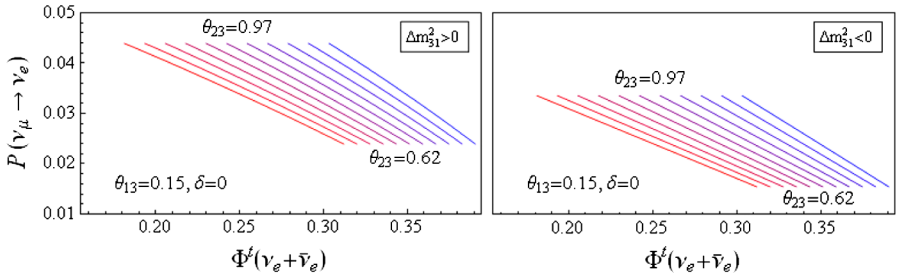

FIG. 6 (color online). The loci for $\theta_{23} \in [0.62, 0.97]$ for various compositions.

tells us that $P_{\mu e} > 0.025$ in the shadow can be compatible with $\Phi^t(\nu_e)$ from a pion source but not with $\Phi^t(\nu_e)$ from a muon-damped source. Figure 6 is an example that predicts the relative composition between a pion source and a muon-damped source, where $\theta_{12} = 0.59$, $\theta_{13} = 0.15$, and $\delta = 0$. The change in color of the curves from blue (rightmost) to red (leftmost) indicates the change in composition from 100% pion source to 100% muon-damped source. Unfortunately, the distinction of the composition by every 10% as in Fig. 6 lies far beyond the practicability, since current sensitivities of detectors are too low to use the strategy in the figure for the precise comparison.

The detected flux which is partially from a pion source and partially from a muon-damped source is expressed in terms of x, the portion of a pion-source flux in the total

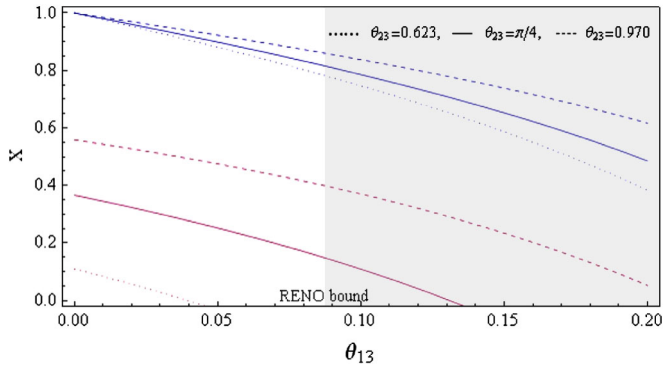

FIG. 7 (color online). The maximum portion of a pion source in a mixed beam which can be distinguished from a pure pion source.

detected ν_e flux,

$$\Phi^t(\nu_e) = x\Phi_p(\nu_e) + (1 - x)\Phi_{md}(\nu_e), \tag{11}$$

where Φ_p is a flux from a pion source and Φ_{md} is a flux from a muon-damped source. Even though the exact value of θ_{13} is known, the undetermined δ limits the composition of a mixed flux or a pure pion-source flux to have blind ranges. Figure 7 describes the maximum portion X of $\Phi_p(\nu_e)$ in a mixed $\Phi^t(\nu_e)$ for various θ_{13} and θ_{23} that can be distinguished from the pure $\Phi_p(\nu_e)$, where $0 < x < X$. The reason for decreasing X as θ_{13} increases is because amplitudes of δ curves become more sizable. The upper (blue) lines are affected only by the range in δ, while the lower (red) lines are affected by systematic uncertainties as well as by δ. The sensitivity of the IceCube detector to astrophysical sources was discussed for neutrinos at TeV to PeV energies [32]. When $\frac{dN_\nu}{dE_\nu}$ is proportional to E^{-2}, the systematic uncertainty is $+10/-15\%$, and when $\frac{dN_\nu}{dE_\nu}$ is proportional to E^{-3}, the systematic uncertainty is $+5/-20\%$. In the case of the E^{-2} spectrum, the composition of a distinguishable mixture from the pure pion-source beam is shown by the lower (red) curves in Fig. 6. Within the current sensitivity of the IceCube detector, a mixed flux with more than 40% (or 20%) pion source cannot be distinguished from a pure pion source when θ_{23} is 0.970 (or $\pi/4$) and θ_{13} reaches the 3σ upper bound at RENO. Within the current upper bound of θ_{13}, as seen in the figure, a pure pion source cannot be distinguished even from a pure muon-damped source, unless $P_{\mu e}$ helps in the identification in such a way as in Figs. 5 and 6.

V. CONCLUDING REMARKS

Neutrino telescopes will detect neutrino beams from astronomical bursts. However, the results will barely be helpful in describing the initial condition of cosmic neutrino beams since the uncertainties in neutrino masses and mixing angles are broad and the fluxes to be measured are sensitive to the masses and the mixing angles. On the other hand, the improvement of the precision in parameters is also hard to attain by using results at a neutrino telescope itself since even an original beam as an initial condition cannot be defined without using the telescope.

Our strategy was to consider the fluxes to be detected at a telescope like IceCube accompanied with oscillation probabilities at a LBL T2K. The expected fluxes were examined for sensitivities to mixing angles, in comparison with the sensitivities of other types of oscillation probabilities to mixing angles. A few restricted cases were presented as examples to show that neutrino fluxes at telescopes may be useful to resolve the degeneracies embedded in terrestrial neutrino oscillations, followed by a discussion on the limit of source identification which is allowed within the sensitivity of IceCube to astrophysical neutrinos.

ACKNOWLEDGMENTS

K. Siyeon thanks Z. Xing for information on neutrino telescopes and thanks physicists at IHEP in Beijing for warm hospitality. This work was supported by the Korea Research Foundation Grant funded by the Korean Government (MOEHRD) (KRF-2005-041-C00108).

[1] Q. R. Ahmad *et al.* (SNO Collaboration), Phys. Rev. Lett. **89**, 011301 (2002).
[2] K. Hirata *et al.* (KAMIOKANDE-II Collaboration), Phys. Rev. Lett. **58**, 1490 (1987).
[3] S. D. Wick, C. D. Dermer, and A. Atoyan, Astropart. Phys. **21**, 125 (2004).
[4] E. Waxman and J. N. Bahcall, Phys. Rev. Lett. **78**, 2292 (1997).
[5] J. P. Rachen and P. Meszaros, Phys. Rev. D **58**, 123005 (1998).
[6] T. Kashti and E. Waxman, Phys. Rev. Lett. **95**, 181101 (2005).
[7] E. Waxman and J. Bahcall, Phys. Rev. D **59**, 023002 (1998).
[8] J. F. Beacom, N. F. Bell, D. Hooper, S. Pakvasa, and T. J. Weiler, Phys. Rev. D **68**, 093005 (2003); **72**, 019901(E) (2005).
[9] T. K. Gaisser, T. Stanev, and G. Barr, Phys. Rev. D **38**, 85 (1988); G. Barr, T. K. Gaisser, and T. Stanev, Phys. Rev. D **39**, 3532 (1989).
[10] M. Honda, K. Kasahara, K. Hidaka, and S. Midorikawa, Phys. Lett. B **248**, 193 (1990); M. Honda, T. Kajita, K. Kasahara, and S. Midorikawa, Phys. Rev. D **52**, 4985 (1995).
[11] Y. Fukuda *et al.* (Kamiokande Collaboration), Phys. Lett. B **335**, 237 (1994).
[12] Y. Fukuda *et al.* (Super-Kamiokande Collaboration), Phys. Lett. B **436**, 33 (1998).
[13] J. Ahrens *et al.* (IceCube Collaboration), Nucl. Phys. B, Proc. Suppl. **118**, 371 (2003).
[14] T. Montaruli *et al.* (ANTARES Collaboration), arXiv: physics/0306057.
[15] J. G. Learned and S. Pakvasa, Astropart. Phys. **3**, 267 (1995).
[16] H. Athar, M. Jezabek, and O. Yasuda, Phys. Rev. D **62**, 103007 (2000); Z. Z. Xing and S. Zhou, Phys. Rev. D **74**, 013010 (2006); W. Winter, Phys. Rev. D **74**, 033015 (2006); K. R. S. Balaji, G. Couture, and C. Hamzaoui, Phys. Rev. D **74**, 033013 (2006); D. Meloni and T. Ohlsson, Phys. Rev. D **75**, 125017 (2007); K. Blum, Y. Nir, and E. Waxman, arXiv:0706.2070; W. Rodejohann, J. Cosmol. Astropart. Phys. 01 (2007) 029.
[17] W. M. Yao *et al.* (Particle Data Group), J. Phys. G **33**, 1 (2006).
[18] M. Maltoni, T. Schwetz, M. A. Tortola, and J. W. F. Valle, New J. Phys. **6**, 122 (2004).
[19] V. Barger, D. Marfatia, and K. Whisnant, Phys. Rev. D **65**, 073023 (2002).
[20] H. Minakata, H. Sugiyama, O. Yasuda, K. Inoue, and F. Suekane, Phys. Rev. D **68**, 033017 (2003); **70**, 059901(E) (2004).
[21] H. Minakata and H. Nunokawa, J. High Energy Phys. 10 (2001) 001.
[22] G. L. Fogli and E. Lisi, Phys. Rev. D **54**, 3667 (1996).
[23] J. Burguet-Castell, M. B. Gavela, J. J. Gomez-Cadenas, P. Hernandez, and O. Mena, Nucl. Phys. **B608**, 301 (2001).
[24] M. C. Gonzalez-Garcia and M. Maltoni, Phys. Rep. **460**, 1 (2008); A. Bandyopadhyay *et al.* (ISS Physics Working Group), arXiv:0710.4947.
[25] G. Barenboim and C. Quigg, Phys. Rev. D **67**, 073024 (2003).
[26] X. Guo *et al.* (Daya Bay Collaboration), arXiv:hep-ex/0701029.
[27] F. Ardellier *et al.* (Double Chooz Collaboration), arXiv: hep-ex/0606025.
[28] K. K. Joo (RENO Collaboration), Nucl. Phys. B, Proc. Suppl. **168**, 125 (2007); S. B. Kim (RENO Collaboration), AIP Conf. Proc. **981**, 205 (2008).
[29] D. S. Ayres *et al.* (NOνA Collaboration), arXiv:hep-ex/0503053.
[30] Y. Itow *et al.* (T2K Collaboration), arXiv:hep-ex/0106019.
[31] M. Lindner, Phys. Scr. **t121**, 78 (2005).
[32] J. Ahrens *et al.* (IceCube Collaboration), Astropart. Phys. **20**, 507 (2004).